Front. Earth Sci. 2015, 9(1): 26–39
DOI 10.1007/s11707-014-0441-z

RESEARCH ARTICLE

Characteristics and genesis of the Feixianguan Formation oolitic shoal reservoir, Puguang gas field, Sichuan Basin, China

Peiyuan CHEN (✉)[1,2], Xiucheng TAN (✉)[1,2], Huiting YANG[2], Ming TANG[2], Yiwei JIANG[3], Xiuju JIN[3], Yang YU[1,2]

1 State Key Laboratory of Oil and Gas Geology and Exploration, Southwest Petroleum University, Chengdu 610500, China
2 School of Geoscience and Technology, Southwest Petroleum University, Chengdu 610500, China
3 Research Institute of Petroleum Exploration and Development, SINOPEC Zhongyuan Oilfield Company, Puyang 457001, China

Abstract The Lower Triassic Feixianguan Formation at the well-known Puguang gasfield in the northeastern Sichuan Basin of southwest China produces a representative oolitic reservoir, which has been the biggest marine-sourced gasfield so far in China (discovered in 2003 with proven gas reserves greater than 350×10^8 m^3). This study combines core, thin section, and scanning electron microscopy observations, and geochemical analysis (C, O, and Sr isotopes) in order to investigate the basic characteristics and formation mechanisms of the reservoir. Observations indicate that platform margin oolitic dolomites are the most important reservoir rocks. Porosity is dominated by intergranular and intragranular solution, and moldic pore. The dolomites are characterized by medium porosity and permeability, averaging at approximately 9% and 29.7 mD, respectively. $^{87}Sr/^{86}Sr$ (0.707536–0.707934) and $\delta^{13}C_{PDB}$ (1.8 ‰–3.5 ‰) isotopic values indicate that the dolomitization fluid is predominantly concentrated seawater by evaporation, and the main mechanism for the oolitic dolomite formation is seepage reflux at an early stage of eodiagenesis. Both sedimentation and diagenesis (e.g., dolomitization and dissolution) have led to the formation of high-quality rocks to different degrees. Dolomite formation may have little contribution, karst may have had both positive and negative influences, and burial dissolution-TSR (thermochemical sulfate reduction) may not impact widely. The preservation of primary intergranular pores and dissolution by meteoric or mixed waters at the early stage of eogenesis are the main influences. This study may assist oil and gas exploration activities in the Puguang area and in other areas with dolomitic reservoirs.

Keywords oolite shoal reservoir, carbonate, diagenesis, Triassic Feixianguan Formation, Puguang gas field, Sichuan Basin

1 Introduction

Marine carbonates account for > 40% of total oil and gas resources in China and form important reservoir rocks in many petroliferous basins, such as the Tarim, Ordos, and Sichuan Basins. The recently discovered Puguang gasfield (2003) in the Sichuan Basin has been the biggest marine-sourced gasfield discovered so far in China. It produces from the Lower Triassic Feixianguan and Upper Permian Changxing formations (Ma et al., 2006a), and is characterized by oolitic and reef dolomites, respectively (Zheng et al., 2011). The Feixianguan oolities here are thick and widespread, with an average thickness of approximately 200 m and up to 443 m (e.g., Puguang 6 well), and are distributed throughout the whole platform margin facies. Although deeply buried (5,000–5,500 m), the reservoirs display relatively high porosity and permeability, with measured core porosity being between 0.3% and 28.8% (average = 9%), and permeability between 0.0004 mD and 2,526 mD (average = 29.7 mD) (Ma et al., 2006b). Thus, the basic characteristics and formation mechanism of this good reservoir has received significant research attention, including the distribution (Wang et al., 2002; Zheng et al., 2011; Tan et al., 2012), origin (Ma et al., 2006a, 2008), diagenesis (Hao et al., 2009; Wang et al.,

Received September 18, 2013; accepted January 9, 2014

E-mail: swpua409@163.com (Peiyuan CHEN), tanxiucheng70@163.com (Xiucheng TAN)

2010; Li et al., 2012), and evolution of pore space (Wang et al., 2009; Zhao et al., 2011) within these sediments. However, the potential origins of this set of reservoirs is still debatable, including dolomitization (Jiang et al., 2013), burial dissolution (commonly associated with thermal sulphate reduction) (Zhu et al., 2005a, b; Ma et al., 2007a), and preservation of primary intergranular pores (Tan et al., 2011). This leads to uncertainty in making exploration and exploitation strategies.

To reduce uncertainty and provide a reference for related studies worldwide, in this paper we address the origin of this set of reservoirs based on a comprehensive investigation of the reservoirs' basic characteristics using new data from systematic coring wells at the Puguang gasfield. The methods are also relatively systematic in general, including comprehensive observations of core, thin section, cast thin-section, cathodoluminescence (CL), and scanning electron microscopy (SEM), together with geochemical examinations (i.e., C, O, and Sr isotopes). The aim is to investigate the basic reservoir characteristics and to evaluate the factors that influence reservoir quality.

2 Geological setting

The Sichuan Basin, located in the northeast of the Sichuan Province, southwest China, is a large intracratonic basin with an area of about 230,000 km^2 (Fig. 1). This basin displays a diamond shape and is surrounded by several mountains, being tectonically bounded by the Longmenshan fold belt in the northwest, the Micangshan uplift in the north, the Dabashan fold belt in the northeast, the Hubei-Hunan-Guizhou fold belt in the southeast, and the Emeishan- Liangshan fold belt in the southwest (Hao et al., 2008) (Fig. 1).

The Sichuan Basin has a complex tectonic and sedimentary history, which leads the basin's having up to 12 km of sediments (Fig. 2(a), Hao et al., 2008). Marine sedimentation dominated from the Precambrian to the Middle Triassic period. The Lower Triassic Feixianguan Formation is 350–700 m thick and can be divided into four general members, Fei-1 (T_1f^1), Fei-2 (T_1f^2), Fei-3 (T_1f^3), and Fei-4 (T_1f^4), from the bottom to the top (Fig. 2). Gas in the studied Puguang gasfield is produced mainly from the Fei-1 and Fei-2 members. The Puguang gas field has the deepest gas reservoirs and highest hydrogen sulphide (15.5%–17%) content of gas fields found so far in the Sichuan Basin (Ma et al., 2007b). The Lower Silurian and Upper Permian sources are the main gas sources, and the thick, basin wide anhydrite beds that occur in the Jialingjiang and Leikoupo formations constitute effective cap rocks for gas accumulation (Fig. 2(b)).

The evolution of the sediments here is closely related to the Kaijiang–Liangping trough, which developed on the margins of the Upper Yangtze Platform (Ma et al., 2006a). The early Fei-1 member inherited the sedimentary framework from the underlying Changxing Formation in general (Zou et al., 2008), forming a platform–trough framework (Fig. 2(b)). The deep water present during this marine transgression, combined with the presence of steep slopes,

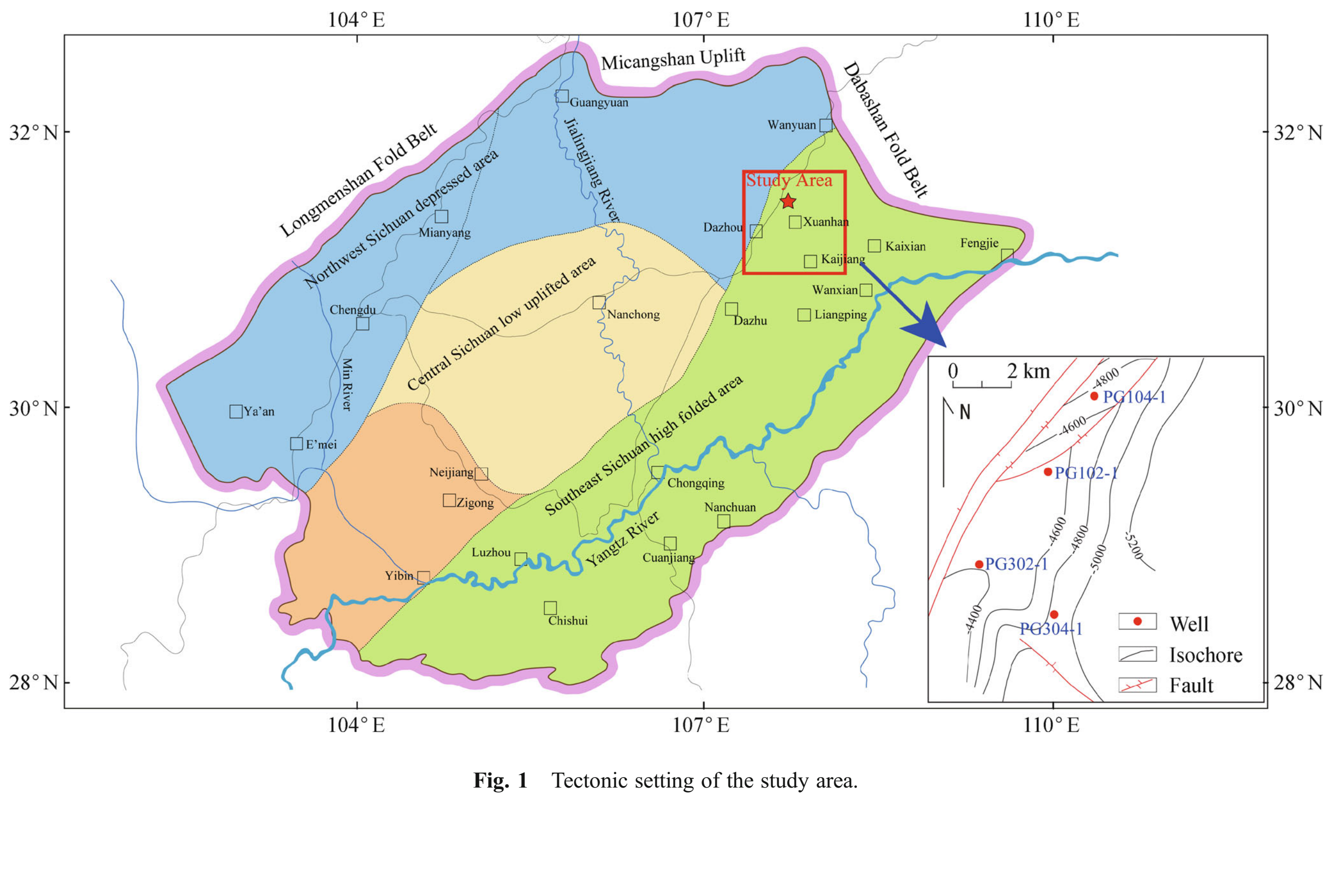

Fig. 1 Tectonic setting of the study area.

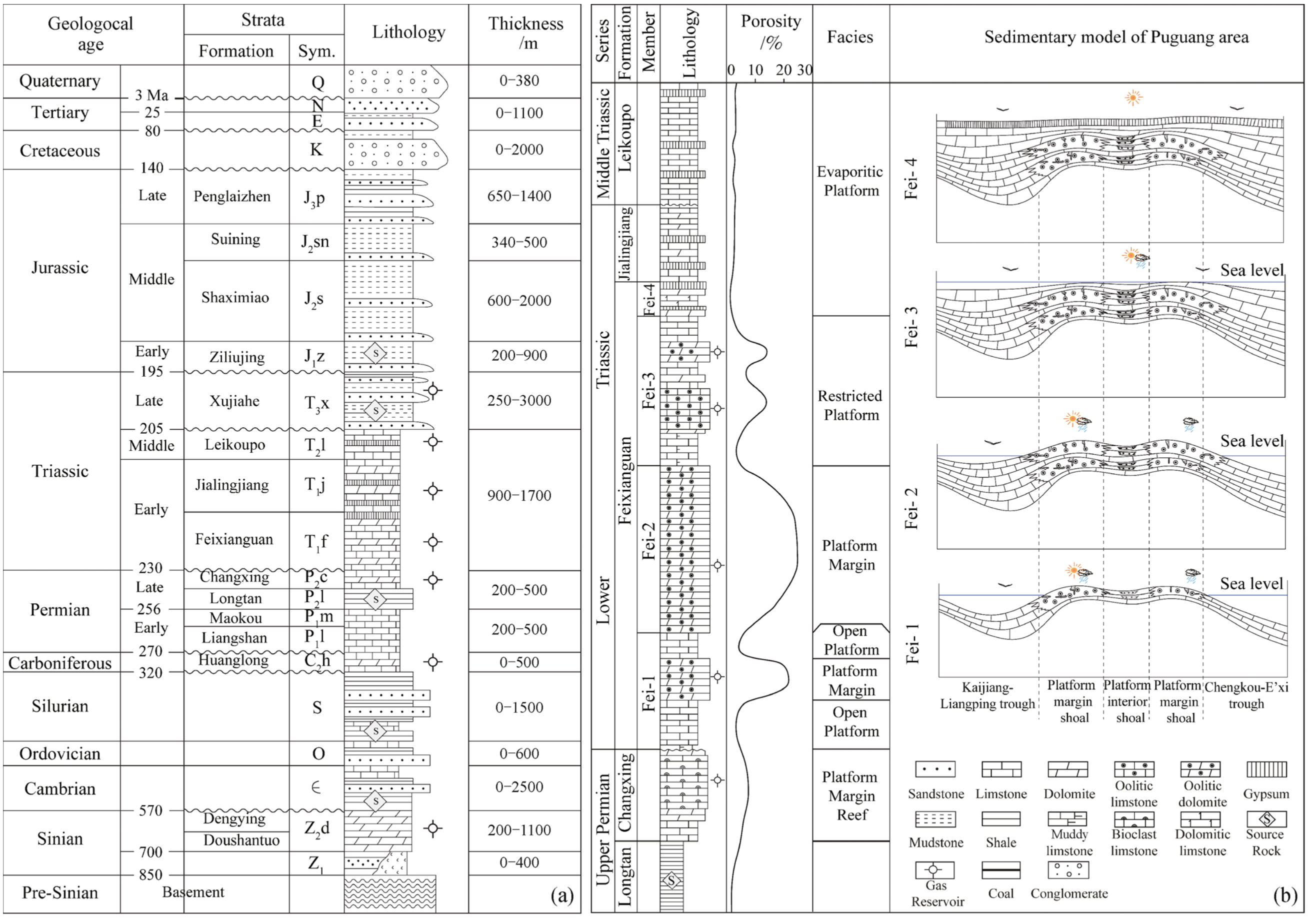

Fig. 2 Generalized stratigraphy and depositional model of the Feixianguan Formation.

resulted in the development of just a few large-scale shoals on the platform margin at this time; some small-scale shoals developed only in tompographic highs (Tan et al., 2012). Collision between the South Qinling orogenic belt and the Upper Yangtze Plate meant that middle–late deposition of the Fei-1 Member and the structure of the study area were strongly affected by collision-induced tectonic deformation (Wang et al., 2007a), a process that reduced the water depth in the study area and allowed the gradual formation of shoals. It is worth noting that sedimentation prograded from the platform margin to the troughs during this period of vertical sedimentation.

The Fei-2 member in the study area still had a two platform–two trough sedimentary framework, but the overall topography of the area changed significantly (Fig. 2(b)), being characterized by an increase in the size of the carbonate platform during sedimentary progradation towards the troughs. In comparison, the Fei-1 period witnessed the development of significant belts of platform-margin facies sediments (Fig. 2(b)). Then, during the Fei-3 period, a short-term marine transgression occurred, associated with the development of platform-margin shoals. The subsequent persistent marine regression that affected the majority of the study area led to subaerial exposure, leading to the study area's having been completely filled and the platform leveled off during the late-stage of the Fei-3 period (Fig. 2(b)); platform interior shoals were developed locally. Then, the entire studied Puguang area was a platform during the Fei-4 period (Fig. 2(b), Ma et al., 2006a).

3 Material and methods

This study was based on samples drawn from four systematic cored wells at the Puguang gasfield, including the Puguang 104-1, 102-1, 302-1, and 304-1 wells (Fig. 1). The cumulative length of the cored well sections is 631 m, and consists primarily of three intervals, Fei 1, Fei 2, and Fei 3. The samples were collected using a combination of petrological and geochemical methods as introduced above. A total of 1,300 samples were selected for thin-section preparation. Thin sections were impregnated with blue- or red-dyed resin, in order to observe the porosity of the rock clearly.

Ten samples from the Puguang 302-1 and 104-1 wells were selected for CL analysis. They were analyzed using the CL8200 MK5 cathodoluminescence microscope

(CLM) in the geological laboratory of the Research Institute of Exploration and Development of the PetroChina Southwest Oil and Gas Field Company.

Eighty six samples from the Puguang 302-1, 104-1, and 102-1 wells were selected for SEM analysis. They were first broken up into fragments, and smooth surfaces were then coated with gold in order to study the mineralogy of the components, cements, textures, and pore systems. The analyzer was an XL30 SEM.

In order to investigate the reservoir porosity and permeability, 2,173 horizontal core plugs from the Puguang 302-1, 104-1, 102-1, and 304-1 wells were analyzed at the geological laboratory of the Research Institute of Exploration and Development of the PetroChina Southwest Oil and Gas Field Company.

Thirty eight samples from the Puguang 302-1 well were selected for carbon (C) and oxygen (O) isotopic analysis, which was performed in the geological laboratory of the Research Institute of Exploration and Development of the PetroChina Southwest Oil and Gas Field Company. The rock samples were ground into powder, passed through a 200-mesh sieve, and dried in an oven. The samples were subsequently reacted with 100% orthophosphoric acid for 24 hours at 25°C in a vacuum system. The C and O isotopic compositions of the obtained CO_2 were measured with a MAT-252 mass spectrometer, and the per-thousand differences in derived C and O isotope levels were calculated using the Pee Dee Belemnite (PDB) standard. The measurement accuracy was 0.1 ‰.

Twenty four samples from the Puguang 302-1 well were collected for strontium (Sr) isotopic analysis, which was performed in the General Resource Development and Environment Analysis and Testing Center of the Guizhou Province. Seventy-milligram samples were crushed until they passed through a 200-mesh sieve and were dissolved in a 0.8 N HCl solution in a Teflon cup for two hours. After centrifugation, the supernatant was passed through an AG50×8 (H^+) cation exchange column, and the pure Sr was washed out using HCl as the eluent. The measurement was performed on a MAT262 solid isotope mass spectrometer. The blank background in the whole process was approximately 2×10^{-10} to 5×10^{-10}, and the error is expressed as 2σ (±).

4 Results

4.1 Basic reservoir characteristics

4.1.1 Lithologies

Visual inspection of more than 1,300 thin sections from cores indicates that platform margins in the Feixianguan Formation reservoir rocks are dominated by dolomites. Lithologies include oolitic, residual oolitic, saccharoidal residual oolitic, crystalline, and arenitic dolomites, of which the oolitic dolomites are the main type and form the uppermost sequence. The oolitic dolomites are medium- to fine-grained and consist mostly (65%–80%) of well-sorted, well-rounded, low-energy ooids (Ma et al., 2006b) with grain sizes of 0.2–1.5 mm (Fig. 3(a)). The ooids are composed of crystalline and micritic dolomite and have undergone local recrystallization.

Interstitial materials within the sediments preserve a complex record of cement generation due to significant dissolution and recrystallization, leading to the development of two or three-generation cements (Fig. 3(b)). Selective dissolution has formed abundant dissolution pores, including numerous intragranular dissolved and oolitic moldic pores (Figs. 3(b)–3(d)). This oolitic dolomite has also been fractured, dissolved, and recrystallized during tectonism, leaving ooid outlines or concentric layers as a so-called “residual” ooliticfabric (Figs. 3(e) and 3(f)).

4.1.2 Reservoir properties

We summarize the petrophysical properties (i.e., porosity and permeability) of the 2,173 core samples from the Feixianguan Formation in Table 1 and Fig. 4. It can be implied that the reservoir rocks are characterized by medium porosities and permeabilities; porosity is 0.3% to 28.8% with an average of 9%, and permeability is 0.0004 mD to 2,526 mD with an average of 29.73 mD. Three porosity-permeability relationships were recognized: a strong positive correlation (Fig. 4(a)), a weak positive correlation in high-porosity and low-permeability reservoir intervals (Fig. 4(b)), and no significant correlation (Fig. 4 (c)).

Additional analysis of thin sections from samples that show each of these three porosity-permeability relationships indicates that samples with positive correlations have reservoir spaces dominated by intergranular dissolved pores, samples with weak positive correlations have reservoir spaces dominated by oolitic moldic and intragranular dissolved pores, and samples with no significant correlation have variable reservoir spaces, with no single pore type being dominant. These differing porosity-permeability relationships are dependent on variations in the types of reservoir space present, indicating that pore structures within Feixianguan Formation reservoirs are quite complex.

4.1.3 Pore types

Thin section core and SEM observations indicate that the Feixianguan Formation oolitic reservoirs are dominated by oolitic moldic, intragranular dissolved, and intergranular dissolved pores (Fig. 3), which account for 90% of the total pore space. Intercrystalline dissolution pores and various micropores account for an additional 4.5% (Fig. 5). The

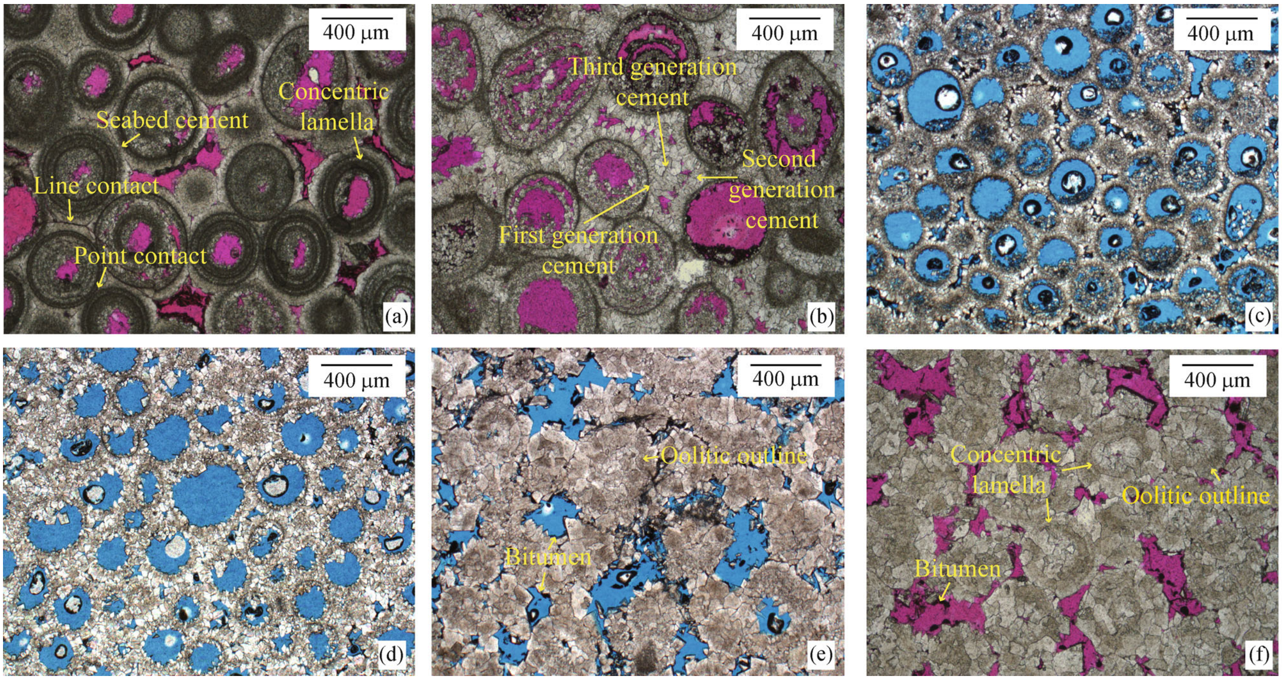

Fig. 3 Photomicrographs showing lithologies of the Lower Triassic Feixianguan Formation. (a) Oolitic dolomite containing densely packed ooids, intragranular dissolved pores, and intergranular dissolved pores; sample from Puguang well 104-1 at a depth of 5,779.83 m, red casting image. (b) Oolitic dolomite with three-generation cement and intragranular dissolved pores; sample from Puguang well 104-1 at a depth of 5,714.33 m, red casting image. (c) Oolitic dolomite with oolitic moldic and intragranular dissolved pores, and residual intergranular pores filled by bitumen; sample from Puguang well 102-1 at a depth of 5,628.28 m, blue casting image. (d) Oolitic dolomite containing oolitic moldic, intragranular dissolved, and rare intergranular dissolved pores, with a pore size of 0.2–0.5 mm; sample from Puguang well 102-1 at a depth of 5,641.96 m, blue casting image. (e) Residual oolitic dolomite containing intergranular dissolved pores that contain bitumen and preserve ooid outlines; sample from Puguang well 102-1 at a depth of 5,669.11 m, blue casting image. (f) Residual oolitic dolomite containing intergranular dissolved pores with bitumen, and preserving ooid outlines and concentric layers; sample from Puguang well 104-1 at a depth of 5,733.61 m, red casting image.

Table 1 Physical parameters of Feixianguan reservoir rock

Well No.	Porosity/%			Permeability/mD		
	Minimum	Maximum	Average	Minimum	Maximum	Average
Puguang 102-1	0.56	28.66	8.93	0.0004	913	11.8
Puguang 104-1	1.1	25.8	9.8	0.0394	2526	85.44
Puguang 302-1	0.3	28.8	9.6	0.0369	648	10.427
Puguang 304-1	0.32	22.65	7.68	0.013	583	11.24

majority of microfissures were filled by carbonaceous mud, sand, and calcite, while a minority were empty or only partly filled. Core observations also indicate that solution pores and vugs formed during eogenetic karstification in the study area (Fig. 6), account for another 4.3% of the total pore space.

4.2 Geochemistry

4.2.1 Sr isotope

The $^{87}Sr/^{86}Sr$ values for the Feixianguan oolitic dolomite are listed in Table 2. Its value is generally distributed from 0.707536 to 0.707934, and the average is 0.707797.

4.2.2 C and O isotopes

C and O isotopic analyses were performed for the Puguang 302-1 well at 5,100–5,400 m. As shown in Table 3 and Fig. 7, the $\delta^{13}C$ value is generally distributed in the range of 1.8 ‰–3.5 ‰, and the average is 2.4 ‰. The $\delta^{18}O$ value is generally between −1.9 ‰ and −5.4 ‰, and the average is −3.8 ‰.

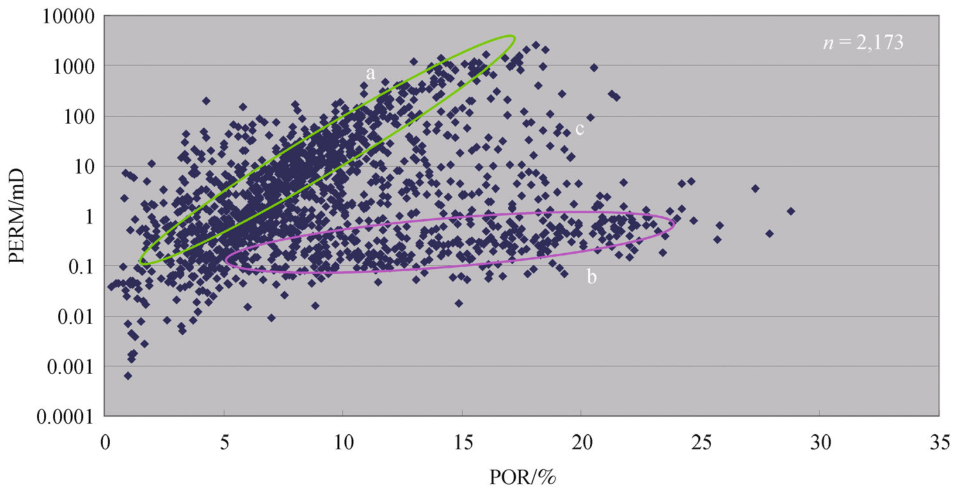

Fig. 4 Relationship between porosity and permeability of the Feixianguan reservoir rock.

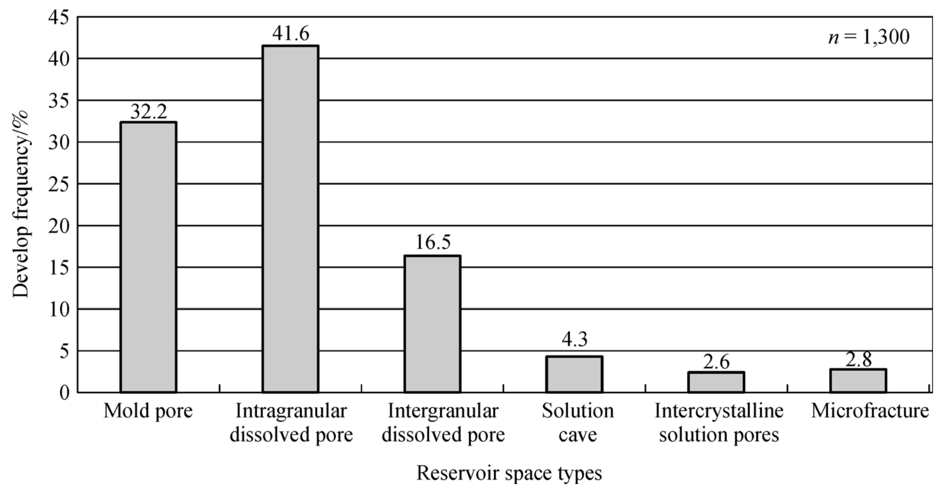

Fig. 5 Development frequency of different reservoir spaces within Feixianguan reservoir rock.

5 Discussion

5.1 The general impact of depositional setting on reservoir formation

Depositional setting is widely acknowledged as fundamental for the development of reservoir rock. Core-derived petrophysical properties of different facies are summarized in Table 4. It is indicated that the physical properties of reservoirs within platform margin shoal facies sediments are more conducive to hydrocarbon reservoir formation than the other microfacies. Inter-shoal sea, lagoon, and tidal flat microfacies sediments are relatively fine grained and do not form effective reservoir rock.

Shoal facies grainstones are relatively resistant to compaction, and rates of porosity decrease during diagenesis are lower than those of finer-grained rocks, leading to the formation of high porosity channels that are ideal for the migration of hydrocarbon or acidic fluids, and indicating that shoal facies grainstones may host late-developing hydrocarbon reservoirs (Brasher and Vagle, 1996). Oolitic shoals were preferentially developed in local topographic highs in the study area (Tan et al., 2012), leading to the formation of oolitic shoals on seafloor highs. Consequently, these shoals are likely to have been subaerially exposed during sea-level falls, leading to interaction with meteoric waters and the development of solution pores, which will be discussed in detail later. Thus, the depositional setting and its primary inter- and/or intra-granular pores provides a foundation for the development of reservoirs.

5.2 Dolomitization and its impact on reservoir formation

The Feixianguan Formation reservoir is dominated by a dolomite reservoir interval, and exploration results indicate

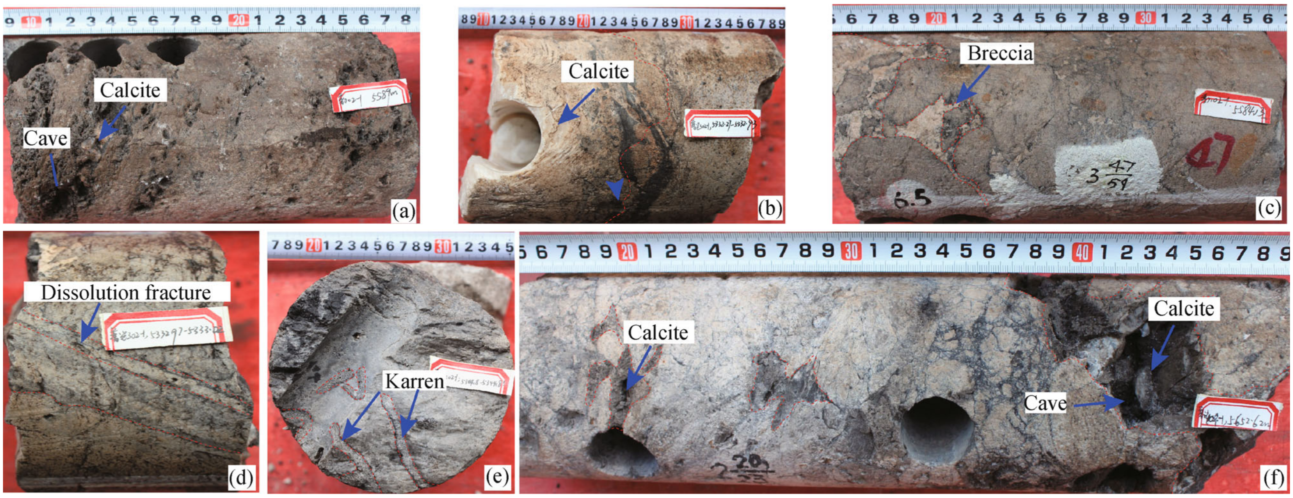

Fig. 6 Characteristics of eodiagenetic karst formation within the Feixianguan carbonates. (a) The Puguang 102-1 well at 5,589.00 m (Fei 1 section), exhibiting oolitic dolomite and the development of mostly horizontal caves that are non-filled to semi-filled with calcite; (b) The Puguang 302-1 well at 5,332.27 m (Fei 1 section), exhibiting oolitic dolomite and large caves that are fully filled with calcite; (c) The Puguang 102-1 well at 5,584.13 m (Fei 2 section), exhibiting oolitic dolomite and the development of karst breccia, with gravels that are sub-angular to angular; (d) The Puguang 302-1 well at 5,332.97 m (Fei 1 section), exhibiting oolitic dolomite and nearly vertical development of dissolution fractures; (e) The Puguang 302-1 well at 5,344.80 m (Fei 1 section), exhibiting oolitic dolomite and karren filled with oolites; (f) The Puguang 104-1 well at 5,652.62 m (Fei 2 section), exhibiting oolitic dolomite and the development of karst breccia and caves, which are filled with calcite and bitumen.

Table 2 Sr isotopic values of the Feixianguan carbonates, Puguang 302-1 well

Depth/m	$^{87}Sr/^{86}Sr$	$2\sigma(\pm)$	Depth/m	$^{87}Sr/^{86}Sr$	$2\sigma(\pm)$
5,283.63	0.707536	0.000013	5,320.15	0.707812	0.000013
5,314.55	0.707789	0.000011	5,320.60	0.70784	0.000012
5,315.25	0.707752	0.000015	5,321.30	0.707883	0.000012
5,315.95	0.707751	0.000013	5,321.83	0.707819	0.00001
5,316.32	0.707775	0.00001	5,322.83	0.707855	0.000011
5,316.52	0.707758	0.000013	5,325.97	0.707934	0.000009
5,316.65	0.707764	0.000009	5,326.95	0.707891	0.000011
5,316.90	0.707763	0.000012	5,362.01	0.707847	0.000012
5,317.02	0.707769	0.000009	5,362.08	0.707892	0.000009
5,317.32	0.707796	0.00001	5,362.65	0.707816	0.00001
5,317.85	0.707923	0.000011	5,363.40	0.707814	0.000012
5,317.92	0.707691	0.000011	5,364.02	0.707646	0.00001

that oolitic dolomites are more conducive to reservoir formation than oolitic limestones, indicating a relationship between dolomitization and reservoir formation.

5.2.1 Dolomitization

The strontium isotopes of the oolitic dolomite are distributed within the range of the global seawater composition of the Early Triassic period ($^{87}Sr/^{86}Sr =$ 0.7072 to 0.7083, Table 2, Korte et al., 2003), indicating seawater influence. This is also supported by the C and O isotopic data, which are generally in the range of normal seawater.

The correlation analysis of C and O isotopes indicates that, as shown in Fig. 7(b), there is a relatively good correlation between the two isotopes, which reflects the impact of diagenesis (Glumac and Spivak-Birndorf, 2002). This diagenesis has little relation to hydrothermal processes, as none of the O isotope values was lower than -10‰, which is commonly indicative of deep-sourced hydrothermal activities (Kaufman and Knoll, 1995).

Table 3 Carbon and oxygen isotopic values of the Feixianguan carbonates, Puguang 302-1 well

Depth/m	δ^{13}C/(PDB ‰)	δ^{18}O/(PDB ‰)	Depth/m	δ^{13}C/(PDB ‰)	δ^{18}O/(PDB ‰)
5,124.69	3.0	−2.0	5,316.12	1.9	−4.5
5,135.26	3.4	−2.4	5,316.52	2.0	−4.5
5,149.00	2.2	−3.7	5,316.65	2.2	−3.6
5,149.38	2.3	−4.6	5,317.32	1.9	−4.2
5,150.27	2.0	−4.9	5,320.60	1.9	−4.4
5,152.66	2.0	−5.1	5,321.30	1.9	−4.6
5,154.25	2.0	−5.2	5,321.83	2.0	−4.4
5,156.37	2.1	−5.1	5,322.83	1.8	−4.4
5,157.00	2.0	−5.3	5,325.97	1.9	−4.9
5,158.24	1.9	−5.3	5,326.95	2.1	−4.8
5,159.06	2.0	−5.4	5,347.26	2.2	−3.4
5,161.39	3.4	−2.2	5,350.35	2.2	−3.5
5,162.55	3.0	−3.0	5,362.01	2.0	−4.5
5,176.54	3.3	−2.2	5,362.65	1.9	−4.5
5,213.67	3.1	−1.9	5,364.02	2.4	−4.2
5,235.18	3.1	−1.9	5,364.45	2.0	−3.7
5,283.63	3.2	−1.9	5,375.20	3.3	−2.0
5,314.55	1.9	−4.3	5,384.00	3.4	−2.2
5,315.95	2.0	−4.4	5,390.32	3.5	−2.1

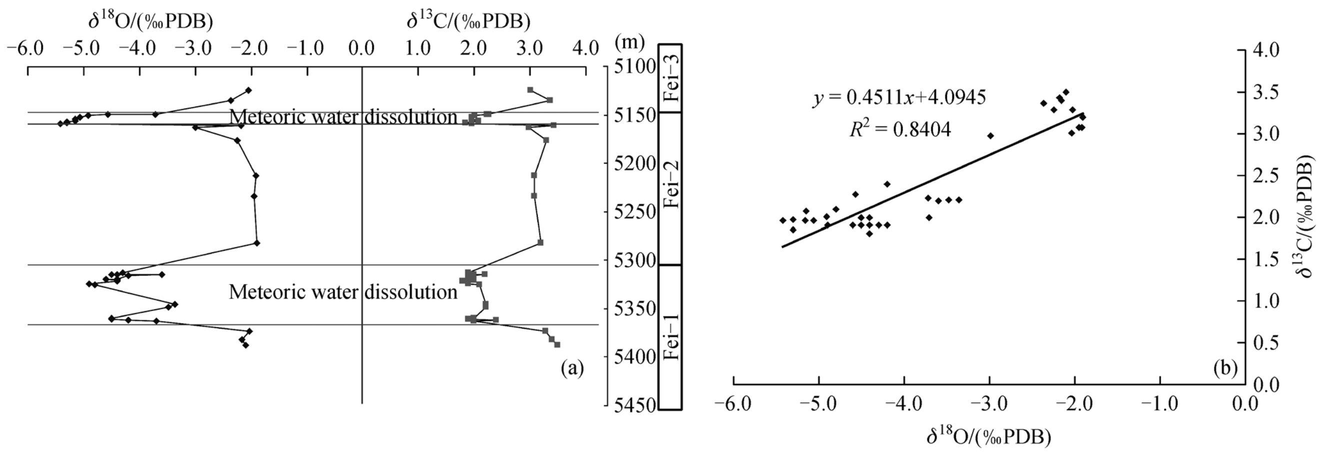

Fig. 7 Carbon and oxygen isotopic variation of the Feixianguan carbonates, Puguang 302-1 well. (a) Correlation between δ^{18}O and δ^{13}C. (b) Data from Table 3.

Table 4 Reservoir physical characteristics of differing sedimentary facies

Sedimentary facies	Porosity/%				Permeability/mD			
	Minimum	Maximum	Average	Sample quantity	Minimum	Maximum	Average	Sample quantity
Platform margin shoal	1.1	28.8	10.7	1295	0.0368	2526	94.76	962
Platform interior shoal	0.56	22	6	292	0.0328	128	4.284	188
Intershoal sea	0.32	3.7	1.7	167	0.0369	9.12	3.87	146
Lagoon	0.45	2.2	0.6	53	0.0004	0.152	0.12	47
Tidal flat	0.3	0.37	0.32	42	0.004	0.131	0.08	39

Considering that the $\delta^{13}C$ value of Triassic seawater is generally 0–1.5 ‰ (Veizer and Hoefs, 1976) and the $\delta^{13}C$ value of 1.8 ‰–3.5 ‰ measured in this study, we infer that the overall fluids in the study area were more salty than seawater at the time of dolomitization (Veizer and Hoefs, 1976). Thus, it can be deduced that the dolomitization fluid would be the evaporative and concentrated seawater, and the dolomitization most likely occurred in semi-closed diagenetic environments. The main formation mechanism of the oolitic dolomites is the seepage reflux in the early diagenetic stage.

5.2.2 Impact of dolomitization on reservoir formation

Approximately 90% of the total pore space of the dolomite reservoir interval in the study area is taken up by oolitic moldic, intragranular, and intergranular pores, in addition to pinhole-like intercrystalline pores within local intervals that were not affected by dissolution. Porosity is generally $< 1\%$ in intervals with intercrystalline pores (Wang et al., 2009), reflecting the approximate intercrystalline pore porosity, and suggesting that dolomitization increased the porosity of these rocks by about 1% within the target reservoir interval. In addition, microscopic observations indicate that preserved structures or structural remnants are present within the oolitic dolomite reservoir interval (Fig. 8(a)), suggesting that dolomitization has involved equal- or near equal-volume metasomatism (Wang et al., 2007b), as few intercrystalline pores formed during volume decrease. SEM imaging of intergranular, oolitic moldic, and intragranular pores indicates that the metasomatized dolomite in the pores is fresh, and that no other residual minerals are located along pore walls (Figs. 8(b) and 8(c)), suggesting that the pores existed prior to dolomitization. These observations indicate that dolomitization has had only a limited impact on pore development in these reservoir rocks.

However, note that although dolomitization did not improve the physical properties largely, it did have an important effect on subsequent diagenesis and pore evolution. This may explain why gas reservoir intervals are generally located within dolomites. Dolomitization of limestone generally changes the permeability, compression resistance, and dissolution characteristics of a reservoir, thereby influencing subsequent reservoir diagenesis and pore evolution (Jiang et al., 2013). Dolomite is more resistant to pressure dissolution than limestone (Duggan et al., 2001; Moradpour et al., 2008), and thus dolomitization may be accompanied by the preservation of existing pores. The resistance of dolomite to pressure dissolution can thus preserve early migration channels, which are then available for late-stage acidic fluids (Warren, 2000). In addition, dolomitization can result in large crystals, causing changes in the pore network and interconnection (Fu et al., 2006).

5.3 Meteoric water dissolution and its impact on reservoir formation

Our core observations revealed that a number of karst features have developed in the carbonates at the top of the Fei 1 and Fei 2 members, such as dissolution fractures, karst caves, and karren (Fig. 6). Karst breccia is one of the important indicators that identify the presence of paleokarst (Gale and Gomez, 2007). The four cored wells in the study area revealed the development of a large number of breccias, e.g., the intervals of 5,583–5,592 m in the Puguang 102-1 well and 5,305–5,363 m in the Puguang 302-1 well (Figs. 6(c) and 6(d)). Cathodoluminescence analyses indicated that the powder-fine crystalline dolomite in the oolitic dolomite near the unconformity interface glows dark red, brown, and purple (Figs. 9(a) and 9(b)), which are distinct characteristics of meteoric water impact (Huang, 1990). Detailed analysis, shown in Fig. 7(a), revealed that the C isotope value of the Puguang 302-1 well, between 5,148–5,160 m (top of Fei 2 member) and 5,305–5,364 m (top of Fei 1 member), is significantly

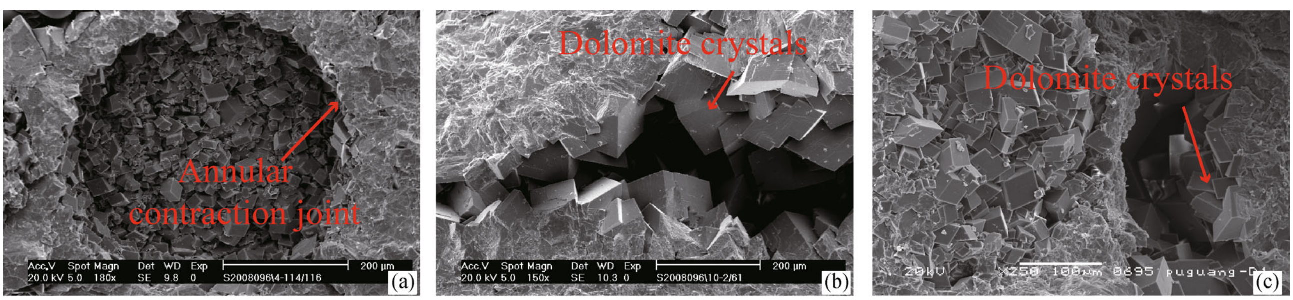

Fig. 8 SEM photomicrographs showing pore type of the Feixianguan reservoir rock. (a) Oolitic dolomite with a well-preserved protolith structure, containing ooids that have undergone complete metasomatism to form finely crystalline dolomite and annular contraction jointing; sample from Puguang well 102-1 at 5,624.79 m. (b) Oolitic dolomite containing crystalline powdery and finely crystalline dolomite along pores and with no relationship to dissolution; sample from Puguang well 102-1 at 5,678.11 m. (c) Oolitic dolomite containing fresh finely crystalline dolomite distributed along pores and not associated with dissolution; sample from Puguang well 302-1 at 5,367.27 m.

smaller than the C isotope value in the upper and lower segments, which indicates that the aforementioned two segments very likely received an input of meteoric water (Meyers et al., 1997).

As for the O isotope, the δ^{18}O value of carbonate can be affected by several complex factors, such as primary seawater temperature and salinity, and it experienced strong fractionation by subsequent diagenesis (Anderson and Arthur, 1983). As shown in Fig. 7(b), the δ^{18}O value decreased in the interval between 5,305 m and 5,364 m, which can be interpreted as the result of the gradually decreasing salinity or increasing temperature of diagenetic fluids (Machel and Lonnee, 2002), or the input of freshwater (Hardie, 1987). When combined with the trend of variation of the C isotopes discussed above, it can be inferred that this effect was primarily caused by a gradual decrease in the salinity of diagenetic fluids due to freshwater input, further supporting the meteoric influences.

Karstification, in theory, may enhance the petrophysical characteristics of carbonate rock due to solution on carbonates (Swei and Tucker, 2012). However, our observations show that the karst development in the Feixianguan Formation in the Puguang area not only produced numerous solution pores and vugs, but also led to the filling of these vugs by fine-grained material (Figs. 6(e) and 6(f)). Microscopic observations show that seepage silt materials occur near karst unconformity (Figs. 9(c) and 9 (d)).

The silt occluding primary and secondary pore spaces and vugs within dolomite is debris which formed in the vadose zone during early diagenesis (Dunham, 1962). This silt reduced the dolomite’s porosity, and divided inter- and intra-granular pores into numerous smaller pore spaces, thereby influencing reservoir permeability. Karst formed during initial subaerial exposure of carbonate units may not increase the total porosity of the sediments (Scholle and Halley, 1985), and porosity may in fact decrease

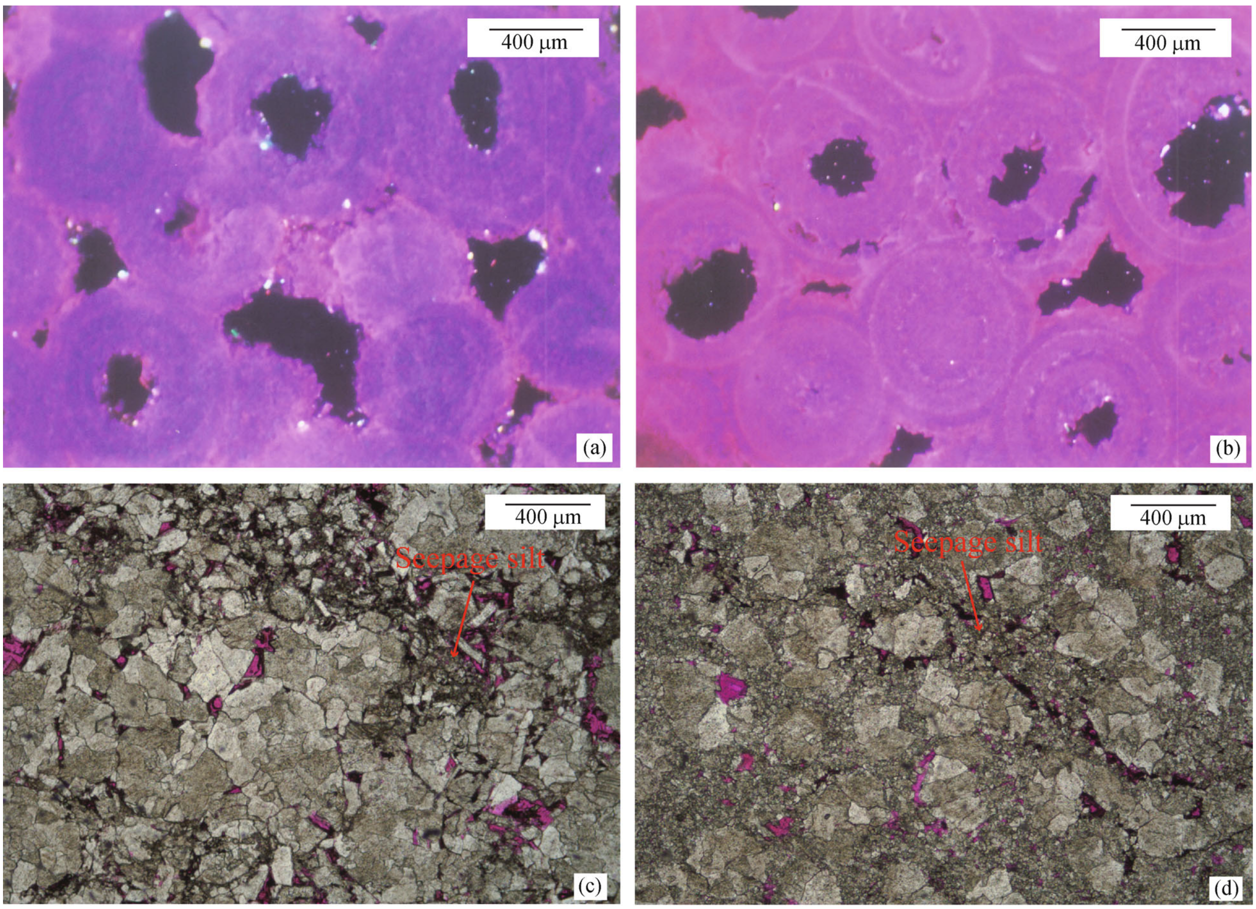

Fig. 9 Photomicrographs showing the karst features developed in the Feixianguan Formation. (a) The Puguang 104-1 well at 5,720.36 m, Fei 1 section, exhibiting residual oolitic dolomite with pore development, mainly involving the formation of intergranular dissolution pores. The dolomite glows purple in cathodoluminescence; (b) The Puguang 102-1 well at 5,587.50 m, Fei 2 section, exhibiting sparry oolitic dolomite with the development of intragranular pores. The dolomite glows purple in cathodoluminescence. (c) The Puguang well 302-1 at 5,325.24 m, karst zone, exhibiting oolitic dolomite containing intergranular dissolved pores filled with seepage silt, red casting thin section. (d) The Puguang well 104-1 at 5,726.41 m, karst zone, exhibiting oolitic dolomite containing intergranular dissolved pores filled with seepage silt, red casting thin section.

(Harrison, 1975; Beach, 1982; Walkden and Williams, 1991). This may be because the karstification and subaerial exposure not only lead to the formation of secondary pores as conventionally thought, but also lead to pore filling with local cements, resulting in the occlusion of original pore spaces (Steinen, 1974; Beach, 1982; Budd, 1988; Walkden and Williams, 1991). Thus, this impact is complex.

Furthermore, three phases of cementation can be identified near the unconformity (Fig. 3(b)). The first phase was formed in a seabed environment, the second was formed during interaction with meteoric water, and the third during burial diagenesis (Wang et al., 2010). Of these three phases of cementation, the second has the most negative impact on reservoir porosity, with the total primary pore space being decreased by 80%–100%. Exposure of oolitic shoal above sea level causes dissolution during interaction with meteoric water, primarily as the ooids are composed of aragonite and high-Mg calcite, both of which are stable in the seabed environment but are unstable during interaction with meteoric water (Moore, 1989). Consequently, unstable minerals are selectively dissolved, resulting in the formation of oolitic moldic and intragranular dissolved pores (Swirydczuk, 1988). In addition, the calcium carbonate produced during aragonite dissolution can be redeposited on grain surfaces to form isopachous rimmed cements that fill primary intergranular pores. This indicates that, although numerous oolitic moldic and intragranular dissolved pores are being formed during ooid dissolution, these pores are generally isolated (Figs. 3(b)–3(d)), radically changing the permeability of the reservoir.

5.4 Burial dissolution associated with thermochemical sulphate reduction (TSR) and its impact on reservoir formation

Burial dissolution associated with thermochemical sulfate reduction (TSR) was thought to be an important influence during the formation of high-quality oolitic shoal reservoirs within Feixianguan Formation sediments in the study area (Zhu et al., 2005a, b; Ma et al., 2007a). Deep fluid-migration channels are needed for TSR to occur, such as early-formed pore layers, faults, joints, fissures, and unconformity planes (Mazzullo and Harris, 1992; Feng et al., 2013), however, the faults, joints and fissures are not widely developed (Tan et al., 2011). Thus, we proposed that the burial dissolution most likely associated with TSR may have little impact on reservoir formation.

In addition, burial dissolution involves balanced chemical reactions, and the TSR reaction equation ($n\mathrm{CaSO_4} + \mathrm{C}_n\mathrm{H}_{2n+2} \rightarrow n\mathrm{CaCO_3} + \mathrm{H_2S} + (n-1)\mathrm{S} + n\mathrm{H_2O}$) indicates that gypsum is required for this process to occur. The syn-depositional marine environment within the study area was high-energy, whereas gypsum generally forms in low-energy environments, such as evaporative salt lakes or lagoons, meaning that it is unlikely that any gypsum layers are present within the platform margin oolitic shoal. This hypothesis is corroborated by the lack of gypsum within Fei-1 and Fei-2 member sediments (Fig. 2).

Furthermore, the TSR reaction is not consistent with the fluid dynamics of sedimentation in the present case. If large-scale TSR did occur, and if overlying sediments (the Fei-4 member contains a large amount of gypsum) or a lagoon to the east of the trough provided $CaSO_4$, then channels must have connected these overlying sediments or the lagoon with the target layer. Dynamic processes mean that hydrocarbon gas generally migrates from high-potential to low-potential zones. Consequently, large-scale TSR in the target layer would cause a problematic dual-direction migration of hydrocarbons, a migration pattern that is difficult to dynamically reconcile with the available evidence, and is hard to interpret in light of the dynamics of this system.

The nature of the TSR chemical reaction means that continuous large-scale TSR can only occur if sufficient reactants and a specific reaction system are present. The Puguang gas field contains abundant hydrogen sulfide (15.5%–17%), indicating that the gas reservoir has not undergone large-scale breaching or destruction, and suggesting that if TSR had occurred, it would have had to occur within a closed system. Even if TSR had produced hydrogen sulfide in this closed system, leading to associated dissolution, equilibrium dissolution-cementation conditions would have been rapidly attained, meaning that significant TSR-related dissolution would have been impossible. Guo and Guo (2012) discussed in detail the possibility of large-scale TSR in the study area using conventional simulation methods, and suggested that TSR did occur, but was not the dominant factor in terms of pore or reservoir formation.

5.5 Preservation of primary intergranular pores and its impact on reservoir formation

Based on the above discussion, it may be suggested that there is another predominant influence upon reservoir formation, not as conventionally thought. Reservoir spaces in the Feixianguan Formation platform margin oolitic shoal reservoir within the Puguang area are dominated by oolitic moldic, intragranular, and intergranular solution pores that account for about 90% of the total pore space. Reservoir conditions vary significantly in differing areas of individual shoals, leading to the centers of the shoals' having better reservoir physical properties (with an average porosity of 12%) than shoal margins (with an average porosity 8%). In addition, as long as the thickness of a single shoal in the study area is > 3 m, the development of intergranular pores would have resulted in the formation of reservoirs dominated by preserved intergranular pores (Tan et al., 2011). Microscopic observations indicate that reservoirs dominated by residual intergranular and enlarged dissolution residual intergranular pores have grains that are in point-line and convex-concave contacts, and only have seabed cements at these grain contacts (Fig. 3(a)). These sediments also contain cements within intergranular pores that do not preserve evidence of dissolution (Fig. 10(a)). Moore and Druckman (1981) and Ehrenberg et al. (2007) indicated that shoal facies reservoirs with primary intergranular pores have grain-supported structures, with low specific compaction, localized seabed cement development at grain boundaries, and the formation of intergranular cement without any evidence of dissolution. This indicates that preservation of primary intergranular pores is an important step in the formation of high-quality oolitic shoal reservoirs in the study area.

This preservation of primary intergranular pores, together with dissolution during interaction with meteoric or mixed waters, contributes to the final development of a relatively good quality reservoir. Regional meteoric-water-related effects are associated with reservoir development (Ma et al., 2006a; Zou et al., 2008; Guo and Guo, 2012), as inter- and intra-granular dissolved and moldic pores only develop at depths affected by meteoric water (Figs. 10(b) and 10(c)). These observations indicate that meteoric-water-related dissolution lasted for a relatively short time. Meteoric water dissolution generally occurs at paleotopographic highs, which are often the developing zones of oolitic shoals; platform margin shoals are associated with vertical accretion (Guo and Guo, 2012). That the tops of shoals are close to sea level means that only limited space is available, and grain shoals can easily be subaerially exposed, leading to the cessation of deposition (Tan et al., 2012). This means that grain shoals that undergo meteoric water dissolution can develop numerous reservoir spaces, such as intragranular dissolved and moldic pores. The exposure of an oolitic shoal within the meteoric water vadose zone causes water to flow downwards into the sedimentary sequence from the upper part of the shoal, meaning that the upper parts of these shoals are easily

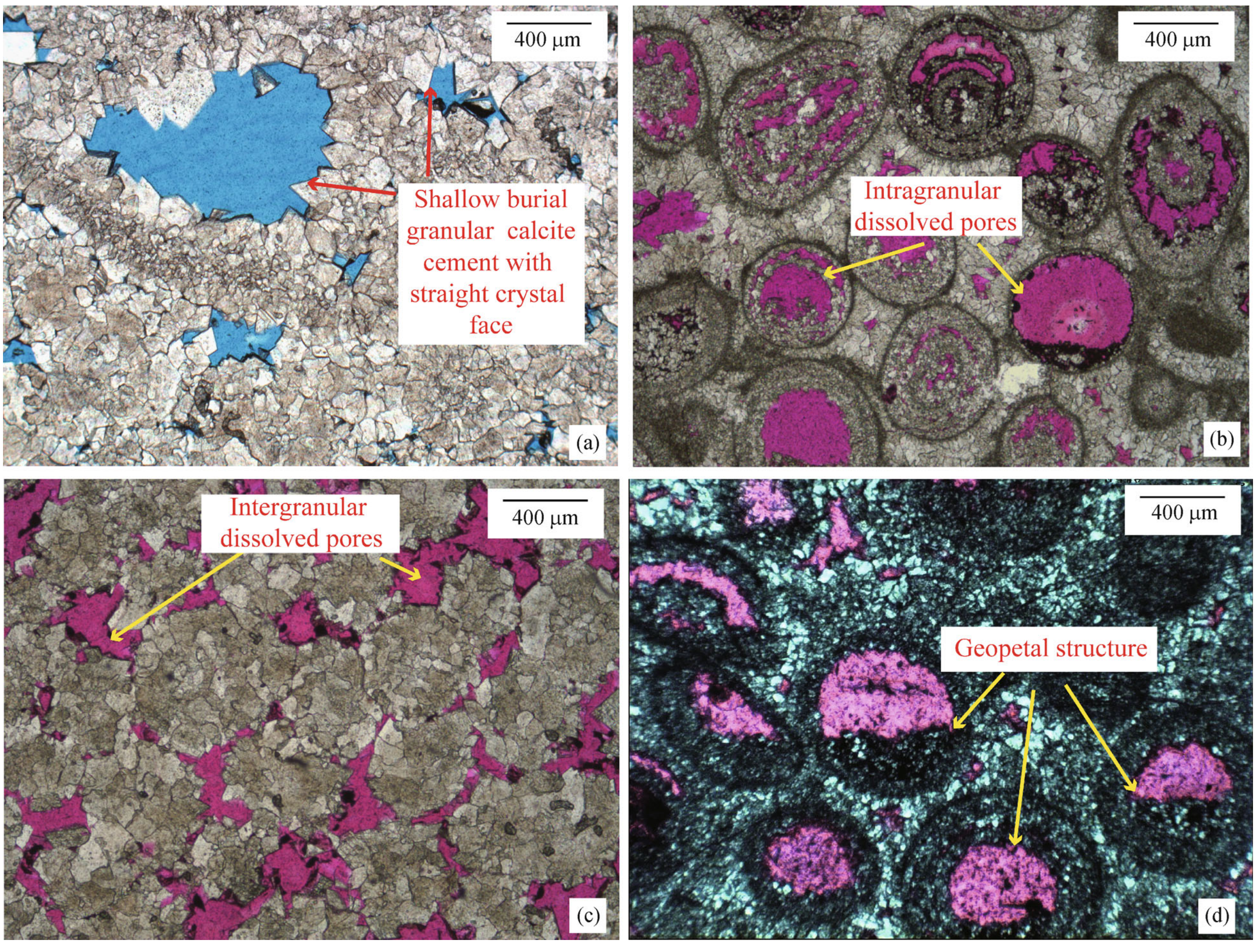

Fig. 10 Photomicrographs showing the importance of preservation of primary intergranular pores in the formation of the Feixianguan reservoir. (a) Oolitic dolomite containing intergranular dissolved pores; sample from Puguang well 102-1 at 5,683.01 m, blue casting thin section. (b) Oolitic dolomite containing intragranular dissolved pores; sample from Puguang well 104-1 at 5,727.38 m, within the meteoric water zone, red casting thin section. (c) Oolitic dolomite containing intergranular dissolved pores; sample from Puguang well 104-1 at 5,731.56 m, within the meteoric water zone, red casting thin section; (d) Oolitic dolomite with intragranular dissolved pores and geopetal structures; sample from Puguang well 302-1 at 5,325.46 m, red casting thin section.

dissolved, whereas the lower parts are not easily dissolved and often preserve primary features (Fig. 10(d), Wang et al., 2010). This means that the majority of reservoir intervals with well-developed pores within the Puguang area platform margin shoal are located on the top or upper parts of the sedimentary sequence, and thus the thickness of the oolitic shoal positively correlates with the thickness of the reservoir.

6 Conclusions

1) The Lower Triassic Feixianguan reservoir rocks in the Puguang gasfield are dominated by platform margin oolitic dolomites. The main reservoir pores are intergranular solution and moldic types. The reservoir has medium porosity (average = 9.0%) and permeability (average = 29.7 mD).

2) The formation mechanism of this relatively good reservoir is complex. Both sedimentation and diagenesis (e.g., dolomitization and dissolution) have impacts to different degrees.

3) Dolomite formation may have little contribution, karst may have had both positive and negative influences, and burial dissolution (i.e., thermochemical sulphate reduction) may not impact widely. The preservation of primary intergranular pores and dissolution by meteoric or mixed waters at the early stage of eogenesis are the main influences.

Acknowledgements We thank the SINOPEC Zhongyuan Oilfield Company for providing the raw data used in this study and for permission to publish this work. This work was supported by the Major State Basic Research Development Program (No. 2012CB214803), China's National Science & Technology Special Project (Grant Nos. 2011ZX05017 and 2011ZX05049), the PetroChina Research Fund (Grant No. 2011D-5006-0105), and the Key Subject Construction Project of Sichuan Province, China (Grant No. SZD 0414). Dr. Jian Cao at Nanjing University is thanked for his enthusiastic support and collaboration during this project.

References

Anderson T F, Arthur M A (1983). Stable isotopes of oxygen and carbon and their application to sedimentologic and paleoenvironmental problems//Arthur M A. Stable Isotopes in Sedimentary Geology, Tulsa. SEPM Short Course, 10: 15–32

Beach D K (1982). Depositional and Diagenetic History of Pliocene-Pleistocene Carbonates of Northwestern Great Bahama Bank: Evolution of A Carbonate Platform. Dissertation for Ph. D degree. Miami: University of Miami, 600

Brasher J E, Vagle K R (1996). Influence of lithofacies and diagenesis on Norwegian North Sea chalk reservoirs. AAPG Bull, 80(5): 746–769

Budd D A (1988). Petrographic products of freshwater diagenesis in Holocene ooid sands, Schooner Cays, Bahamas. Carbonates and Evaporites, 3(2): 143–163

Duggan J P, Mountjoy E W, Stasiuk L D (2001). Fault-controlled dolomitization at Swan Hills Simonette oil field (Devonian), deep basin west-central Alberta, Canada. Sedimentology, 48(2): 301–323

Dunham R J (1962). Classification of carbonate rocks according to depositional texture. In: Han W E, ed. Classification of Carbonate Rocks. AAPG Mem, 1: 108–121

Ehrenberg S N, Nadeau P H, Aqrawi A A M (2007). A comparison of Khuff and Arab reservoir potential throughout the Middle East. AAPG Bull, 91(3): 275–286

Feng J L, Cao J, Hu K, Peng X Q, Chen Y, Wang Y F, Wang M (2013). Dissolution and its impacts on reservoir formation in moderately to deeply buried strata of mixed siliciclastic-carbonate sediments, northwestern Qaidam Basin, northwest China. Mar Pet Geol, 39(1): 124–137

Fu Q L, Qing H R, Bergman K M (2006). Early dolomitization and recrystallization of carbonate in an evaporite basin: the Middle Devonian Ratner laminite in southern Saskatchewan, Canada. J Geol Soc London, 163(6): 937–948

Gale J F W, Gomez L A (2007). Late opening-mode fractures in karst-brecciated dolostones of the Lower Ordovician Ellenburger Group, west Texas: recognition, characterization, and implications for fluid flow. AAPG Bull, 91(7): 1005–1023

Glumac B, Spivak-Birndorf M L (2002). Stable isotopes of carbon as an invaluable stratigraphic tool: an example from the Cambrian of the northern Appalachians, USA. Geology, 30(6): 563–566

Guo X S, Guo T L (2012). Exploration Theory and Practice of Large Scale Carbonate Platform Margin Gas Field of Puguang and Yuanba. Beijing: Science Press, 159–163 (in Chinese)

Hao F, Guo T L, Du C G, Zou H Y, Cai X Y, Zhu Y M, Li P P, Wang C W, Zhang Y C (2009). Accumulation mechanisms and evolution history of the giant Puguang gas field, Sichuan Basin, China. Acta Geol Sin, 83(1): 136–145

Hao F, Guo T L, Zhu Y M, Cai X Y, Zou H Y, Li P P (2008). Evidence for multiple stages of oil cracking and thermochemical sulfate reduction in the Puguang gasfield, Sichuan Basin, China. AAPG Bull, 92(5): 611–637

Hardie L A (1987). Dolomitization: a critical view of some current views. J Sediment Res, 57(1): 166–183

Harrison R S (1975). Porosity in Pleistocene Grainstones from Barbados: some preliminary observations. Bull Can Pet Geol, 23(2): 383–392

Huang S J (1990). Cathodoluminescence and diagenetic alteration of marine carbonate minerals. Sedimentary Geol and Tethyan Geol, 4: 9–15

Jiang L, Cai C F, Worden R H, Li K K, Xiang L (2013). Reflux dolomitization of the Upper Permian Changxing Formation and the Lower Triassic Feixianguan Formation, NE Sichuan Basin, China. Geofluids, 13(2): 232–245

Kaufman A J, Knoll A H (1995). Neoproterozoic variations in the C-isotopic composition of seawater: stratigraphic and biogeochemical implications. Precambrian Res, 73(1–4): 27–49

Korte C, Kozur H W, Bruckschen P, Veizer J (2003). Strontium isotope evolution of Late Permian and Triassic seawater. Geochim Cosmochim Acta, 67(1): 47–62

Li K K, Cai C F, Jiang L, Cai L L, Jia L Q, Zhang B, Xiang L, Yuan Y Y (2012). Sr evolution in the Upper Permian and Lower Triassic carbonates, northeast Sichuan basin, China: constraints from chemistry, isotope and fluid inclusions. Appl Geochem, 27(12):

2409–2424

Ma Y S, Mou C L, Guo X S, Yu Q, Tan Q Y (2006a). Sedimentary facies and distribution of reservoir rocks from the Feixianguan Formation in the Daxian-Xuanhan region, NE Sichuan. Acta Geol Sin, 80(1): 137–151

Ma Y S, Guo T L, Cai X Y (2006b). Petroleum geology of the Northeastern Sichuan Basin and the characteristics of Puguang Gas Field, China. AAPG International Conference (Perth, Australia) Technical Program

Ma Y S, Guo T L, Zhao X F, Cai X Y (2008). The formation mechanism of high-quality dolomite reservoir in the deep of Puguang Gas Field. Sci China Ser D, 51(S1): 53–64

Ma Y S, Guo T L, Zhu G Y, Cai X Y, Xie Z Y (2007a). Simulated experiment evidences of the corrosion and reform actions of H_2S to carbonate reservoirs: an example of Feixianguan Formation, east Sichuan. Chin Sci Bull, 52(S1): 178–183

Ma Y S, Guo X S, Guo T L, Huang R, Cai X Y, Li G X (2007b). The Puguang gas field: new giant discovery in the mature Sichuan Basin, southwest China. AAPG Bull, 91(5): 627–643

Machel H G, Lonnee J (2002). Hydrothermal dolomite-a product of poor definition and imagination. Sediment Geol, 152(3–4): 163–171

Mazzullo S J, Harris P M (1992). Mesogenetic dissolution; its role in porosity development in carbonate reservoirs. AAPG Bull, 76(5): 607–620

Meyers W J, Lu F H, Zachariah J K (1997). Dolomitization by mixed evaporative brines and freshwater, upper Miocene carbonates, Nijar, Spain. J Sediment Res, 67(5): 898–912

Moore C H (1989). Carbonate Diagenesis and Porosity. New York: Elsevier, 338

Moore C H, Druckman Y (1981). Burial diagenesis and porosity evolution, upper Jurassic Smackover, Arkansas and Louisiana. Am Assoc Pet Geol Bull, 65(4): 597–628

Moradpour M, Zamani Z, Moallemi S A (2008). Controls in reservoir quality in the Lower Triassic Kangan Formation, Southern Persian Gulf. J Pet Geol, 31(4): 367–385

Scholle P A, Halley R B (1985). Burial diagenesis: out of sight, out of mind. In: Schneidermann N, Harris P M, eds. Carbonate Cements. Society of Economic Paleontologists and Mineralogists Special Publication, 36: 309–334

Steinen R P (1974). Phreatic and vadose diagenetic modification of Pleistocene limestone: petrographic observations from subsurface of Barbados, West Indies. AAPG Bull, 58(6): 1008–1024

Swei G H, Tucker M E (2012). Impact of diagenesis on reservoir quality in ramp carbonates: Gialo Formation (Middle Eocene), Sirt Basin, Libya. J Pet Geol, 35(1): 25–47

Swirydczuk K (1988). Mineralogical control on porosity type in Upper Jurassic Smackover ooid grainstones, Southern Arkansas and Northern Louisiana. J Sediment Petrol, 58(2): 339–347

Tan X C, Liu H, Li L, Luo B, Liu X G, Mou X H, Nie Y, Xi W Y (2011). Primary intergranular pores in Oolitic Shoal Reservoir of Lower Triassic Feixianguan Formation, Sichuan Basin, Southwest China: fundamental for reservoir formation and retention diagenesis. Journal of Earth Science, 22(1): 101–114

Tan X C, Zhao L Z, Luo B, Jiang X F, Cao J, Liu H, Li L, Wu X B, Nie Y (2012). Comparison of basic features and origins of oolitic shoal reservoirs between carbonate platform interior and platform margin locations in the Lower Triassic Feixianguan Formation of the Sichuan Basin, Southwest China. Petroleum Science, 9(4): 417–428

Veizer J, Hoefs J (1976). The nature of $^{18}O/^{16}O$ and $^{13}C/^{12}C$ secular trends in sedimentary carbonate rocks. Geochim Cosmochim Acta, 40(11): 1387–1395

Walkden G M, Williams O (1991). The diagenesis of the late Dinantian Derbyshire-East Midland carbonate shelf, central England. Sedimentology, 38(4): 643–670

Wang F, Lu X X, Lo C H, Wu F Y, He H Y, Yang L K, Zhu R X (2007a). Post-collisional, potassic monzonite–minette complex (Shahewan) in the Qinling Mountains (central China): $^{40}Ar/^{39}Ar$ thermochronology, petrogenesis, and implications for the dynamic setting of the Qinling orogen. J Asian Earth Sci, 31(2): 153–166

Wang S Y, Jiang X Q, Guan H L, Bao Y J (2009). Pore evolution of reservoirs of Feixianguan Formation in Puguang gas field in Northeastern Sichuan. Petroleum Geology & Experiment, 31(1): 26–30 (in Chinese)

Wang S Y, Jiang X Q, Guan H L, Bao Y J (2010). Diagenesis effects of Lower Triassic Feixianguan Formation reservoir in Puguang gas field, Northeast Sichuan. Petroleum Geology & Experiment, 32(4): 366–372 (in Chinese)

Wang X Z, Zhang F, Ma Q, Yang M P, Wang Y G, Wen Y C, Yang Y, Zhang J (2002). The characteristics of reef and bank and the fluctuation of sea-level in Feixianguan Formation period of Late Permian-Early Triassic, East Sichuan basin. Acta Sedimentologica Sinica, 20(2): 249–254 (in Chinese)

Wang Y G, Wen Y C, Hong H T, Xia M L, He T T, Song S J (2007b). Diagenesis of Triassic Feixianguan Formation in Sichuan Basin, Southwest China. Acta Sedimentologica Sinica, 25(6): 831–839 (in Chinese)

Warren J (2000). Dolomite: occurrence, evolution and economically important associations. Earth Sci Rev, 52(1–3): 1–81

Zhao W Z, Xu C C, Wang T S, Wang H J, Wang Z C, Bian C S, Li X (2011). Comparative study of gas accumulations in the Permian Changxing reefs and Triassic Feixianguan oolitic reservoirs between Longgang and Luojiazhai-Puguang in the Sichuan Basin. Chin Sci Bull, 56(31): 3310–3320

Zheng R C, Dang L R, Wen H G, Chen Z W, Chen F M, Zhang H J (2011). Diagenesis characteristics and system for dolostone in Feixianguan Formation of Northeast Sichuan. Earth Science-Journal of China University of Geoscience, 36(4): 659–669 (in Chinese)

Zhu G Y, Zhang S C, Liang Y B, Dai J X, Li J (2005a). Isotopic evidence of TSR origin for natural gas bearing high H_2S contents within the Feixianguan Formation of the northeastern Sichuan Basin, southwestern China. Sci China Ser D, 48(11): 1960–1971

Zhu G Y, Zhang S C, Liang Y B, Dai J X, Li J (2005b). Origins of high H_2S-bearing natural gas in China. Acta Geol Sin, 79(5): 697–708

Zou H Y, Hao F, Zhu Y M, Guo T L, Cai X Y, Li P P,Zhang X F (2008). Source rocks for the Giant Puguang Gas Field Sichuan Basin: implication for petroleum exploration in marine sequences in South China. Acta Geologica Sinica, 82(3): 477–486